Heliyon 10 (2024) e39166

Contents lists available at ScienceDirect

Heliyon

journal homepage: www.cell.com/heliyon

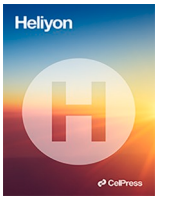

Research article

# New application of ombuoside in protecting auditory cells from cisplatin-induced ototoxicity via the apoptosis pathway

Xingxing Wu [a], Xixia Peng [b], Yue Zhang [c], Wanjun Peng [a], Xiaochan Lu [d], Tingting Deng [a], Guohui Nie [a,*]

[a] *Shenzhen Key Laboratory of Nanozymes and Translational Cancer Research, Department of Otolaryngology, Shenzhen Institute of Translational Medicine, Shenzhen Second People's Hospital, The First Affiliated Hospital of Shenzhen University, Guangdong Key Laboratory for Biomedical Measurements and Ultrasound Imaging, National-Regional Key Technology Engineering Laboratory for Medical Ultrasound, School of Biomedical Engineering, Shenzhen University Medical School, Shenzhen, 518035, China*

[b] *Center for Protein and Cell-Based Drugs, Institute of Biomedicine and Biotechnology, Shenzhen Institutes of Advanced Technology, Chinese Academy of Sciences, Shenzhen, 518055, China*

[c] *Department of Otolaryngology, Shaanxi Provincial People's Hospital, Xi'an, 710068, China*

[d] *Department of Otorhinolaryngology, Peking University Shenzhen Hospital, Shenzhen, 518036, China*

A R T I C L E I N F O

*Keywords:*
Ombuoside
Cisplatin
Ototoxicity
Reactive oxygen species
Apoptosis

A B S T R A C T

Hearing loss is caused by many factors including ototoxic drug-induced hair cell damage. Ombuoside, an antioxidant isolated from *Gynostemma pentaphyllum*, has been suggested to serve as a new neuroprotective drug. However, the role of ombuoside in protecting inner ear hair cells from ototoxic drug-induced damage has not been investigated. Here, we demonstrated the protective potential of ombuoside in mitigating drug-induced ototoxicity *in vivo* and *in vitro*. We used cisplatin, a highly ototoxic anti-tumor drug, to induce hair cell damage. Our results showed that ombuoside significantly increased the survival of cisplatin-treated HEI-OC1 cells. Further mechanism research suggested that ombuoside protects HEI-OCI cells from cisplatin-induced apoptosis by reducing the cisplatin-induced upregulation of apoptosis-promoting proteins Bax, Bak, as well as apoptosis indicator proteins cytochrome C and cleaved-caspase-3, and the downregulation of apoptosis-inhibiting proteins Bcl-2. Ombuoside also protects the cells from the excessive ROS production and mitochondrial membrane depolarization triggered by cisplatin. These results demonstrated the potential for ombuoside in protecting hair cells from cisplatin by suppressing ROS generation and the mitochondrial apoptotic cascade. Ombuoside showed promise in protecting hair cells from cisplatin-induced apoptosis by suppressing ROS generation and the mitochondrial apoptotic cascade. Furthermore, ombuoside co-treatment in mouse cochlear explants and zebrafish lateral neuromasts rescued the decreased number and deformed morphology of hair cells resulting from cisplatin exposure. These findings further validated our conclusions and indicated that ombuoside is a potential protector against hearing loss caused by ototoxicity as a clinical side effect of cisplatin.

* Corresponding author.
*E-mail addresses:* wuxiaodouaran05@163.com (X. Wu), pengxixia1990@163.com (X. Peng), zhangyue6968@163.com (Y. Zhang), wanjun0330@163.com (W. Peng), xiaochanlu@pku.edu.cn (X. Lu), dttmuye@163.com (T. Deng), nieguohui@email.szu.edu.cn (G. Nie).

https://doi.org/10.1016/j.heliyon.2024.e39166
Received 14 May 2024; Received in revised form 6 October 2024; Accepted 8 October 2024
Available online 9 October 2024

## 1. Introduction

Hearing loss is a common sensory disorder in humans. The World Health Organization (WHO) has reported that >5 % of the global population (corresponding to approximately 70 million people) experiences disabling hearing loss, defined as hearing impairments of moderate to high severity. Among these individuals, 34 million are children [1,2]. Hearing loss primarily results from hair cell damage, which can be caused by many factors, such as ototoxic drugs, excessive noise, aging, and genetic diseases. More than 600 drugs are ototoxic, among which, aminoglycoside antibiotics and platinum-containing chemotherapeutic agents are the most extensively researched [3–5]. Cisplatin, a platinum-based compound, is a highly effective anti-tumor drug that is widely used to treat various types of cancer. However, it is highly ototoxic [4,6,7]. 40 %–80 % of adults and >50 % of children that received cisplatin treatment suffered from permanent hearing loss after cisplatin treatment [4,7].

The ototoxicity that induced by cisplatin can be caused by various factors and mechanisms, including apoptosis, oxidative stress damage, autophagy and inflammation [8–10]. At present, the primary cause of cisplatin ototoxicity is believed to be cisplatin induced reactive oxygen species (ROS) [8,11–14]. Low levels of ROS produced by cells under normal physiological conditions have strong chemical activity in signal transduction [15–17]. To maintain redox homeostasis, cells neutralize excess ROS via the antioxidant system. Functional disruption of the intracellular antioxidant system can lead to excessive ROS production and disrupt the cellular structure through various mechanisms, including DNA damage, increased lipid peroxidation of the cell membrane, and others [15,17]. Cisplatin induces excessive ROS production in the cochlea and promotes the activation of caspase-3. This leads to apoptosis of the hair cells and spiral ganglion neurons in the organ of Corti, ultimately resulting in hearing loss [18].

Many efforts have been explored to reduce the adverse effects of cisplatin, including the development of small-molecule drugs, improvement of delivery methods, as well as updating of drug delivery systems [8,15,19] Otoprotective drugs such as amifostine, N-acetylcysteine, and sodium thiosulfate have been shown to protect against cisplatin-induced hearing loss [20–23]. To date, only sodium thiosulfate is approved by the FDA to prevent cisplatin induced hearing loss of children [24]. Cisplatin predominantly triggers ototoxicity by inducing the generation of ROS, while antioxidants effectively neutralize these ROS. Hence, it is crucial to identify more antioxidants that mitigate the ototoxic adverse effects of cisplatin.

Flavonoid is a kind of well-known antioxidants, function effectively as scavengers of free radicals [25,26]. A dietary flavonol, quercetin (3,5,7,3′,4′-pentahydroxy flavone) has been documented to reduce oxidative stress in streptozotocin-induced diabetic rats and to protect against cisplatin-induced apoptotic cell death in zebrafish [27,28]. The flavonol glycoside ombuoside is isolated from *Gynostemma pentaphyllum* and exhibits multiple pharmacological effects [29–33]. Its low toxicity and broad range of pharmacological effects have garnered significant research interest. Moreover, ombuoside improves chronic stress-induced anxiety in mice, suggesting its potential as a therapeutic approach for the treatment of anxiety disorders [29,30,32]. Notably, ombuoside mitigates the cytotoxicity of L-3, 4-dihydroxyphenylalanine (L-DOPA) in dopaminergic neurons [30,31]. L-DOPA is the most effective and commonly prescribed therapy for treating Parkinson's disease. However, excessive dosages and prolonged usage of L-DOPA might cause adverse effects, including motor fluctuations, dyspnea, and emotional disturbances [34,35]. Ombuoside improves the adverse effects of L-DOPA in parkinson's, suggesting that it may be a new neuroprotective drug. This neuroprotective effect may be attributed to its ability to reduce L-DOPA-induced ROS levels and apoptosis [30,31]. Since the increasing ROS and apoptosis is the main cause of cisplatin induced ototoxic adverse effects, this indicating a potential role of ombuoside in reduce cisplatin-induced ototoxicity. However, the protective role of ombuoside against ototoxicity has not been investigated and needs to be explored as yet.

Here, we investigated for the first time the protective effects of ombuoside against cisplatin-induced ototoxicity. Our findings provide significant experimental evidence for the potential clinical use of ombuoside in the treatment of drug-induced hearing loss.

## 2. Materials and methods

### 2.1. HEI-OC1 cell culture

HEI-OC1 cells derived from the organ of Corti of the transgenic Immortomouse™ were gifted by Professor Huawei Li at Fudan University (Shanghai, China). Cultures were grown in high-glucose Dulbecco's Modified Eagle Medium (DMEM, 11965-084, Gibco) with 10 % fetal bovine serum (FBS, 10099-141, Gibco) at 33 °C and 5 % $CO_2$, without antibiotics. HEI-OC1 cells were seeded at $5 \times 10^3$ cells per well in 96-well plates or $2 \times 10^5$ per well in 6-well plates.

### 2.2. Zebrafish husbandry

AB strain zebrafish were cultured in circulating water at a constant temperature of 28 °C following a 14-h light/10-h dark cycle. The transgenic strain *Tg(brn3c:GFP)* was gifted by Professor Huawei Li at Fudan University (Shanghai, China). The zebrafish used in this study were all at 5 days post fertilization.

### 2.3. Cochlear explant culture

C57BL/6 mice were decapitated with scissors after anesthesia on postnatal day 3 (P3), and the cochlear tissue was dissected in 0.01 mmol/L phosphate-buffered saline (PBS). The detailed operation was performed as described previously [36,37]. The cochlear explants were cultured in DMEM/F12 medium (SH30023.01, Thermo Scientific) supplemented with N2/B27 (17502-048/17504-44, Invitrogen) and ampicillin (P0781, Sigma-Aldrich) at 37 °C in 5 % $CO_2$.

### 2.4. Drug treatment

Ombuoside was dissolved in Dimethyl Sulfoxide (DMSO) to prepare 10 mmol/L stock solutions, then diluted in the culture medium to their respective working concentrations, ensuring that the final DMSO concentration was kept below 1 %. Cisplatin was stored as a 1 mM solution in PBS and diluted to a final concentration of 30 μM (for HEI-OC1 cells and cochlear explants based on our previous study) or 800 μM (for zebrafish based on previous study) in the culture medium for the experiments [37,38].

In the experiment involving the screening of ombuoside concentrations, HEI-OC1 cells were treated with varying concentrations (0, 5, 10, 20, 30, 40, 80, or 100 μmol/L) of ombuoside for 24h.

HEI-OC1 cells or cochlear explants were divided into such four groups randomly: untreated (control), cisplatin (30 μmol/L), ombuoside (30 μmol/L), and ombuoside and cisplatin (30 μmol/L each) co-treatment. The cisplatin groups and ombuoside groups were treated with cisplatin or ombuoside, respectively, for 24 h. The co-treated group was pretreated with ombuoside for 2 h, and then co-treated with cisplatin and ombuoside for 24 h.

The zebrafish were randomly divided into four groups (90 individuals in each group): untreated (control), cisplatin (800 μmol/L), ombuoside (30 μmol/L), and ombuoside (30 μmol/L) and cisplatin (800 μmol/L) co-treatment. The cisplatin groups and ombuoside groups were treated with cisplatin or ombuoside for 8 h, respectively. The co-treated group was pretreated with ombuoside for 2 h, and then co-treated with cisplatin and ombuoside for 8 h.

All zebrafish experiments (accession number: IACUC-2023-8793-01) and mouse cochlear explant cultures (accession number: 202300226) were conducted in accordance with the Guiding Principles for the Care and Use of Laboratory Animals approved by The First Affiliated Hospital of Shenzhen University (Shenzhen Second People's Hospital).

### 2.5. Cell viability assay

The viability of HEI-OC1 cells after drug treatment was measured using the cell counting kit-8 (CCK-8) assay according to the manufacturer's instructions (CK04, Dojindo Laboratories). Briefly, HEI-OC1 cells were seeded at $5 \times 10^3$ cells per well in 96-well plates and incubated overnight. Post-treatment, a 10 % CCK-8 solution in DMEM was added and incubated at 37 °C for 2 h. Optical density (OD) at 450 nm was measured using a plate reader.

### 2.6. Flow cytometry

After drug treatment, the HEI-OC1 cells were digested using ethylenediaminetetraacetic acid (EDTA)-free 0.25 % trypsin (In Hank's Balanced Salt Solution) and collected. Flow cytometry was performed according to the instructions provided with the Annexin V-fluorescein isothiocyanate/propidium iodide (FITC/PI) apoptosis detection kit (4A Biotech, Beijing, China). Specifically, the cells were resuspended in 1 × binding buffer and incubated with Annexin V-FITC for 5 min in the dark then stained with PI before loading to a BD Accuri C6 flow cytometer (BD Biosciences, USA).

### 2.7. Western blotting

Drug-treated HEI-OC1 cells were digested with EDTA-free 0.25 % trypsin and collected. Proteins were extracted using lysis buffer (P0013C, Beyotime) containing protease inhibitors (04693159001, Roche) and phosphatase inhibitors (49068370001, Roche). The BCA Protein Assay Kit (Thermo, 23225) was used to measure protein concentrations. Next, 10 μg of protein and loading buffer were heated at 95 °C for 10 min to denature the proteins, and then separated on 10 % polyacrylamide gels and transferred to PVDF membranes. Subsequently, the membranes were blocked for 1 h at room temperature with 5 % nonfat dry milk in 1 × TBST. Following blocking, the membranes were incubuted overnight at 4 °C in 1 × TBST with 2 % BSA and primary antibodies for Bax (D2E11) rabbit monoclonal antibody (mAb) (1:1000, 5023T, Cell Signaling Technology), Bak (D4E4) rabbit mAb (1:1000, 12105T, Cell Signaling Technology), B-cell lymphoma-extra large (Bcl-2) (D17C4) rabbit mAb (1:1000, 3498T, Cell Signaling Technology), cytochrome *c* (136F3) rabbit mAb (1:1000, 4280T, Cell Signaling Technology), and beta-tubulin rabbit mAb (1:1000, ab6046, Abcam). After washing the membranes with 1 × TBST and then were incubated with secondary antibody was goat anti-rabbit IgG H&L (horseradish peroxidase [HRP]) (1:5000, ab6721, Abcam) at room temperature for 1 h. Fianlly, afert washing with 1 × TBST, the membranes were incubated with Immobilon® ForteWestern HRP Substrate (WBLUF0100, Millipore), and protein bands were visualized using Amersham lmager 680.

### 2.8. Mitochondrial membrane potential (MMP) and ROS detection

After washing drug-treated HEI-OC1 cells with 1 × PBS, MMP and ROS detection were performed using different kits according to the manufacturer's protocol. MMP was measured using 100 nmol/LMitoTracker® Red (40741ES50, YEASEN) with an incubation period of 30 min at 37 °C. Total ROS were measured using 5 μmol/L CellRox Green (C10444, Thermo Fisher) for 30 min at 37 °C, while mitochondrial ROS were assessed using 5 μmol/L MitoSOX Red (M36008, Thermo Fisher) with a 10-min incubation at 37 °C, respectively. After 1 × PBS washing, the sample was mounted with VECTASHIELD® mounting medium (H-1000, Vector) and imaged on a ZEISS LSM 800 confocal microscope.

### 2.9. Immunofluorescence

Drug-treated HEI-OC1 cells, cochlear explants, and zebrafish were fixed with 4 % paraformaldehyde for 1 h, washed with PBS, and permeabilized with 1 % Triton X-100 for 30 min. The samples were then blocked with 10 % bovine serum albumin for 1 h, followed by incubation with primary antibodies overnight at 4 °C. After washing three times with PBS, the cells were incubated with fluorescence-conjugated secondary antibodies at room temperature for 3h. Cell nuclei of the HEI-OC1 cells, cochlear explants, and zebrafish were stained with 1 μg/mL 4′,6-diamidino-2-phenylindole (DAPI, D8417, Sigma) at room temperature for 30min. After immunofluorescence, the sample was mounted with VECTASHIELD® mounting medium (H-1000, Vector) and imaged on a ZEISS LSM 800 confocal microscope by using 488 nm and 561 nm excitation lasers respectively.

The primary antibodies Cleaved-Caspase 3 polyclonal antibody (1:1000 dilution, 9661S, CST) was used in HEI-OC1 cells, GFP polyclonal antibody (1:1000 dilution, A11122, Invitrogen) was used in zebrafish, and myosin VIIa rabbit polyclonal antibody (1:400 dilution, 25–6790, Proteus Biosciences) was used in cochlear explants. The secondary antibody was Alexa Fluor 488-labeled donkey anti-rabbit antibody (1:1000 dilution, A21206, Invitrogen).

### 2.10. Terminal deoxynucleotidyl transferase dUTP nick end labeling (TUNEL) assay

TUNEL assays were performed on cochlear explants that were first subjected to drug treatment and subsequent immunofluorescence staining. The In Situ Cell Death Detection Kit (11684795910, Roche) was conducted according to the manufacturer's protocol. The TUNEL of drug-treated cochlear explants were performed after IF. Briefly, cochlear explants stained with 100 μL TUNEL mixture for 1 h at 37 °C in a dark atmosphere. A positive control was prepared by treating the sample with 100 μL DNase I (EN0521, Thermo) before fixation, while a negative control was set up by adding the labeling solution without TUNEL transferase to the sample. The sample was mounted with VECTASHIELD® mounting medium (H-1000, Vector) and imaged on a ZEISS LSM 800 confocal microscope by using 488 nm and 561 nm excitation lasers respectively.

### 2.11. Real-time quantitative polymerase chain reaction (RT-qPCR)

RT-qPCR was used to detect the relative mRNA levels in different groups of zebrafish treated with drugs. Thirty individuals were pooled in each sample. Total RNA was extracted using TRIzol (15596-026, Invitrogen). After removing DNA with DNase I, the cDNA was generated by reverse transcription kit (TRT-101, ToYoBo). The 20 μl reverse transcription reaction, containing 1 μg of RNA, 5 μM Oligo dT primer, 1 mM deoxynucleotide triphosphate mixture, and 100U of ReverTra Ace, was incubated at 42 °C for 60 min, followed by 95 °C for 10 min. Finally, the target genes were amplified using the cDNA as a template. RT-qPCR was performed using SYBR Green Master Mix (QPK-201, ToYoBo): 2 × SYBR Green real-time master mix, 10 μL; cDNA, 1 μL; Forward primer, 1 μL; Reverse primer, 1 μL; $H_2O$, 7 μL. The PCR amplification conditions were: 95 °C for 2min; 40 cycles × (95 °C for 15s; 60 °C for 20 s; 72 °C for 30s); 65 °C for 0.05s; 95 °C, 0.5s. The relative mRNA levels were analyzed using the $2^{-\triangle\triangle CT}$ method. The primers used for qPCR in this study were listed in Supplementary Table 1.

### 2.12. Statistical analysis

The data were analyzed in GraphPad Prism9 and displayed as mean ± standard error of the mean (SEM). One-way analysis of variance (ANOVA) followed by a Dunnett multiple comparisons test was performed for multiple group comparison. A p value $\leq 0.05$ was statistically significant. For each HEI-OC1 cell culture experiments contained at least 3 independent biological replicates. For cochlear explant culture and zebrafish experiments, each group contained at least 3 independent cochlear explants or zebrafishes. Each experiment was repeated at least three times.

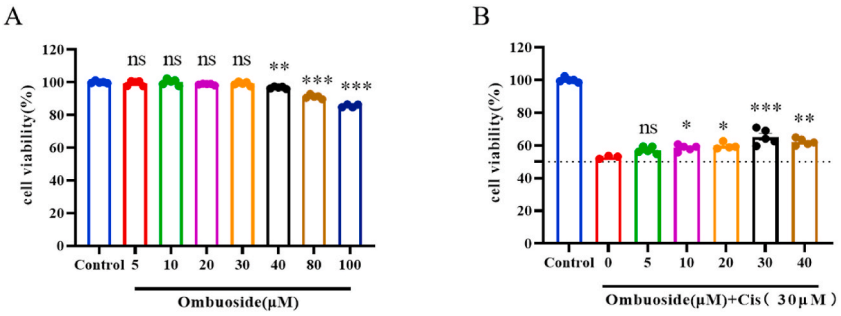


**Fig. 1.** Ombuoside protects HEI-OC1 cells from cisplatin toxicity. A. HEI-OC1 cells were treated with varying concentrations of ombuoside doses for 24 h. Cell viability was analyzed by cell counting kit-8 (CCK-8) and compared with untreated cells, N ≥ 5 B. HEI-OC1 cells were pre-treated with varying concentrations of ombuoside for 2 h and then co-treated with 30 μmol/L cisplatin for 24 h. Cell viability was evaluated by CCK-8 and compared with cells treated with cisplatin alone, N ≥ 4. Data are presented as mean ± SEM. *P ≤ 0.05, **P ≤ 0.01, ***P ≤ 0.001, and ****P ≤ 0.0001.

## 3. Results

### 3.1. Ombuoside reduces cisplatin-induced damage to HEI-OC1 cells

HEI-OC1 is one of the few cell lines available for studying hearing and has been extensively utilized in studies related to autophagy, aging, and cellular protective mechanisms [39]. In this study, we employed HEI-OC1 cells as a model to study drug-induced ototoxicity. We first verified whether ombuoside affects the growth of HEI-OC1 cells. The cells were treated with 0, 5, 10, 20, 30, 40, 80, or 100 μmol/L of ombuoside for 24 h. Only treatment with 80 or 100 μmol/L ombuoside inhibited cell growth (Fig. 1A).

To investigate the protective effects of ombuoside against cisplatin-induced damage, HEI-OC1 cells were pretreated with 0, 5, 10, 20, 30, or 40 μmol/L of ombuoside for 2 h and then exposed to ombuoside and 30 μmol/L cisplatin co-treatment for 24 h. The CCK8 results showed cell survival rates of 52.85 ± 0.5533 %, 57.19 ± 0.8988 %, 58.52 ± 0.8542 %, 59.73 ± 1.007 %, 65.25 ± 2.085 %, and 62.28 ± 0.9170 %, respectively, for 0, 5, 10, 20, 30, and 40 μmol/L of ombuoside (Fig. 1B). Thus, ombuoside significantly increased the survival of cisplatin-treated HEI-OC1 cells, with the 30 μmol/L dose demonstrating the most protective effect. These results suggest the protective role and optimal concentration of ombuoside against cisplatin-induced cytotoxicity in HEI-OC1 cells.

### 3.2. Ombuoside reduces cisplatin-induced apoptosis in HEI-OC1 cells

Flow cytometry showed a survival rate of cells treated with 30 μmol/L cisplatin alone of 52.17 ± 0.3844 %. However, when co-treated with ombuoside, the survival rate increased to 84.73 ± 0.3283 % (Fig. 2A and B) Therefore, ombuoside significantly reduced cisplatin-induced death and apoptosis of HEI-OC1 cells.

To further investigate the impact of ombuoside on cisplatin-induced apoptosis, we analyzed the apoptotic signaling pathway using western blotting. After cisplatin treatment, expression of apoptosis-promoting signaling proteins, including Bax, Bak, increased significantly, while those of apoptosis-inhibiting indicator proteins Bcl2, decreased significantly (Fig. 2C and D). When co-treated with ombuoside, the expression of Bax and Bak, significantly decreased compared with that in cells treated with cisplatin alone, whereas the expression of Bcl2 increased (Fig. 2C and D). Additionally, we observed a significant increase in the expression of cytochrome *c*, an indicator of apoptosis. Cytochrome *c* activates caspase-8, caspase-9, and caspase-3 in the endogenous apoptotic pathway [40,41]. Caspase-3, a key factor in caspase cascade-induced apoptosis, may be one of the final executors of apoptotic events. Our results showed that the signals of cytochrome *c* and caspase-3 significantly increased after cisplatin treatment but decreased significantly when co-treated with ombuoside (Fig. 2C–D, Fig. 3A–D, and Fig. 3Q). Additionally, staining with DAPI is adequate to assessing apoptosis at a morphological level, including chromatin condensation, nuclear deformation [42]. Moreover, DAPI staining showed that the number

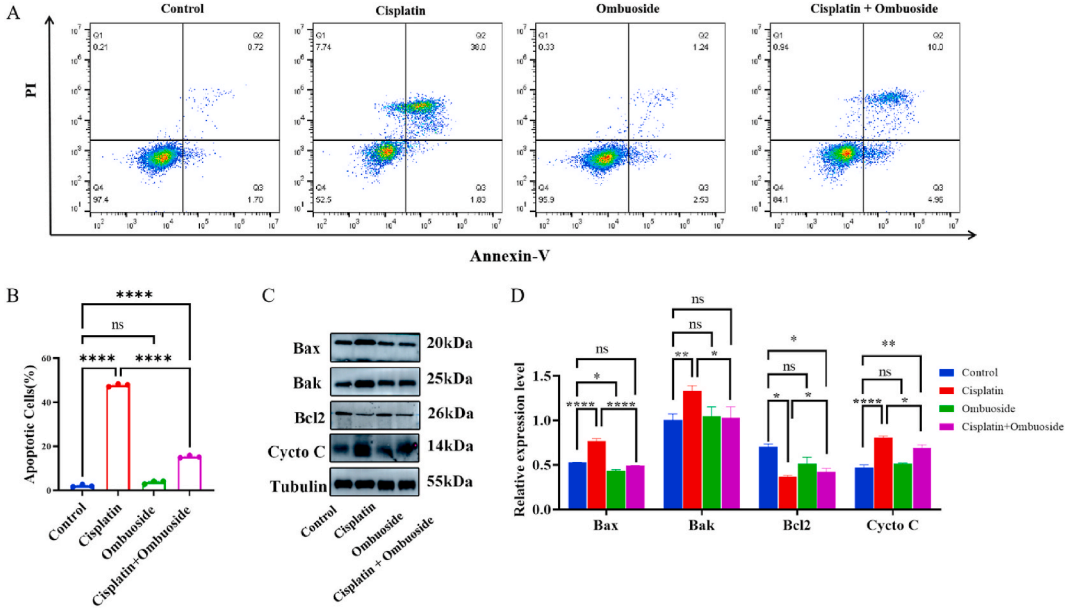


**Fig. 2.** Ombuoside protects HEI-OC1 cells against cisplatin-induced apoptosis. A. Cell apoptosis analysis by flow cytometry. Negative auto-fluorescence control (using untreated cells without dyes) and positive controls (using fixed untreated cells stained with AX or PI) were employed to set the parameters of the cytometer. Comparison between cells treated with cisplatin alone and co-treated with ombuoside, N = 3. The upper right quadrant (Q2) represents apoptotic cells. B. Quantification of apoptotic cells in Fig. 2A, N = 3. Data are presented as mean ± SEM. ****P ≤ 0.0001. C. Western blot showing the expression of apoptosis-associated proteins in HEI-OC1 cells treated with cisplatin alone and co-treated with ombuoside using tubulin as a reference. (The non-adjusted blot image is included in supplementary material) D. Quantification of protein expression in Fig. 2C. Data are presented as mean ± SEM. *P ≤ 0.05, **P ≤ 0.01, ***P ≤ 0.001, and ****P ≤ 0.0001.

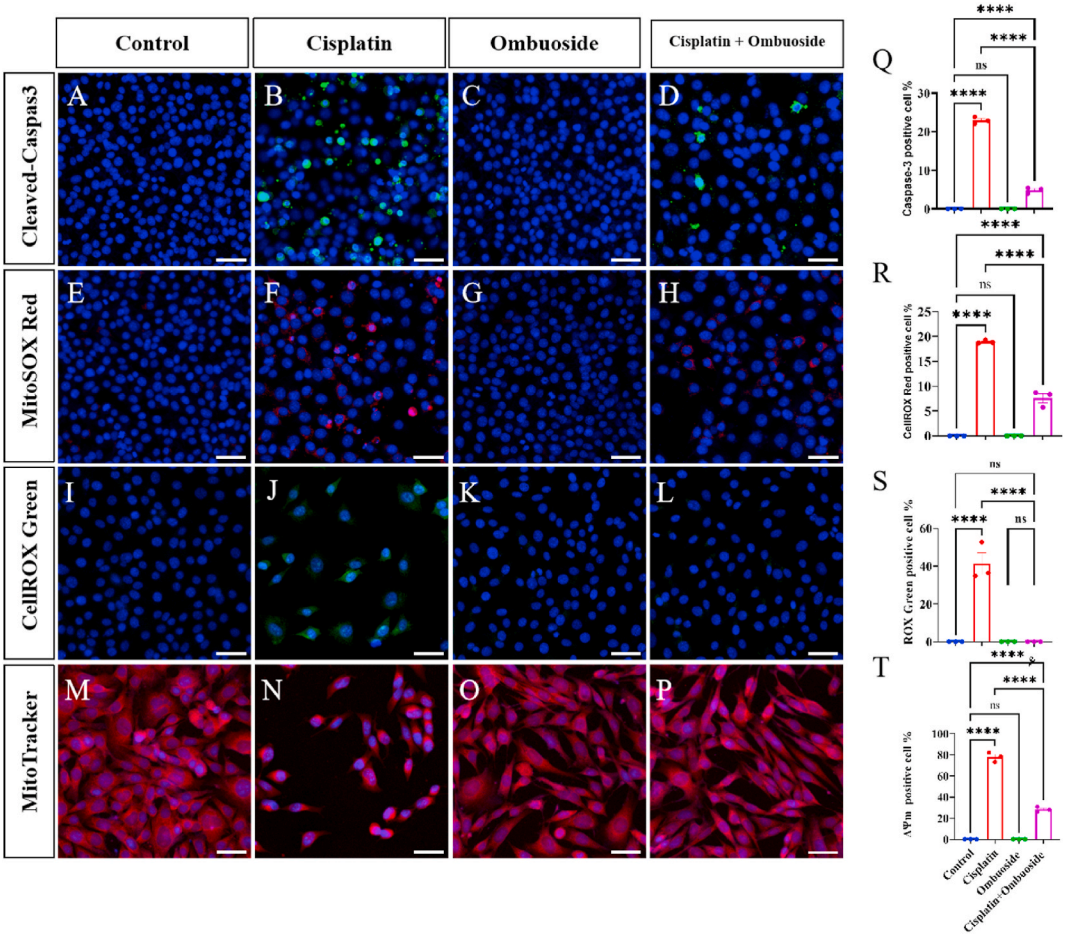


**Fig. 3.** Ombuoside protects HEI-OC1 cells against cisplatin-induced reactive oxygen species (ROS) and mitochondrial membrane potential (MMP). A–D. Immunofluorescence detection of apoptotic cells by staining for cleaved caspase 3 (green) and nuclei (blue)by 4′,6-diamidino-2-phenylindole (DAPI), N = 3.E–H. Detection of mitochondrial ROS (mtROS) levels using MitoSOX Red vmtROS (red), N = 3. I–L. Measurement of intracellular total ROS (green) using a CellROX Green probe, N = 3. M − P Measurement of the MMP using MitoTracker® Red probe (red), N = 3. Scale bar: 50 μm. Q-T. Quantification of positive cell in Fig. .3A–P. The percentage value was obtained from the ratio of positive cell number to total cell number in the same view field at the same magnification by manually counting. Data are presented as mean ± SEM. ****P ≤ 0.0001.

of apoptotic cells in cisplatin treatment was significantly higher than that in co-treated with ombuoside (Figs. S1A–E). These results suggest that ombuoside protects HEI-OC1 cells from cisplatin-induced cell death by inhibiting the apoptotic pathway.

### *3.3. Ombuoside reduces cisplatin-induced oxidative stress in HEI-OC1 cells*

Cisplatin-induced ROS production leads to cell apoptosis [39,43]. To investigate the potential of ombuoside to reduce cisplatin-induced apoptosis by inhibiting ROS production, we assessed the intracellular and mitochondrial ROS levels in HEI-OC1 cells using CellROX Green and MitoSOX Red staining. We observed few CellROX Green-positive cells and MitoSOX Red-positive cells in both the control and ombuoside-treated groups. Intracellular and mitochondrial ROS levels increased significantly after cisplatin treatment. However, cells co-treated with ombuoside and cisplatin exhibited significantly decreased intracellular and mitochondrial ROS levels (Fig. 3E–H, 3I–L, Fig. 3R and S). Accumulation of ROS causes mitochondrial depolarization, leading to the release of cytochrome *c*, which ultimately activates caspase-8, caspase-9, and caspase-3 in the endogenous apoptotic pathway. The loss of mitochondrial membrane potential (ΔΨm) is a signal of mitochondrial damage [44,45]. We used MitoTracker Red staining to detect the mitochondrial membrane potential. In the control group, the mitochondrial membrane of HEI-OC1 cells showed obvious probe aggregation and displayed strong red fluorescence signal. The red fluorescence reduced significantly in cells exposed only to cisplatin, indicating the mitochondrial membrane experienced depolarization. While co-treated with ombuoside, the mitochondrial damage caused by cisplatin exposure was alleviated, as evidenced by increased red fluorescence compared with cisplatin exposure only (Fig. 3M–P, Fig. 3T). These results suggest that ombuoside reduces cisplatin-induced apoptosis via the mitochondria-related apoptotic pathway.

### 3.4. Ombuoside protects cochlear explants from cisplatin-induced hair cell damage

In the untreated group, cochlear explants contained a neatly arranged layer of inner hair cells and three layers of outer hair cells. The arrangement of inner and outer hair cells in the ombuoside group was well-organized, with no significant difference in the number of hair cells (base: 70.0 ± 2.45, middle: 84.5 ± 0.96, apex: 79.3 ± 1.45) (Fig. 4C–G, K), compared with that in the untreated group

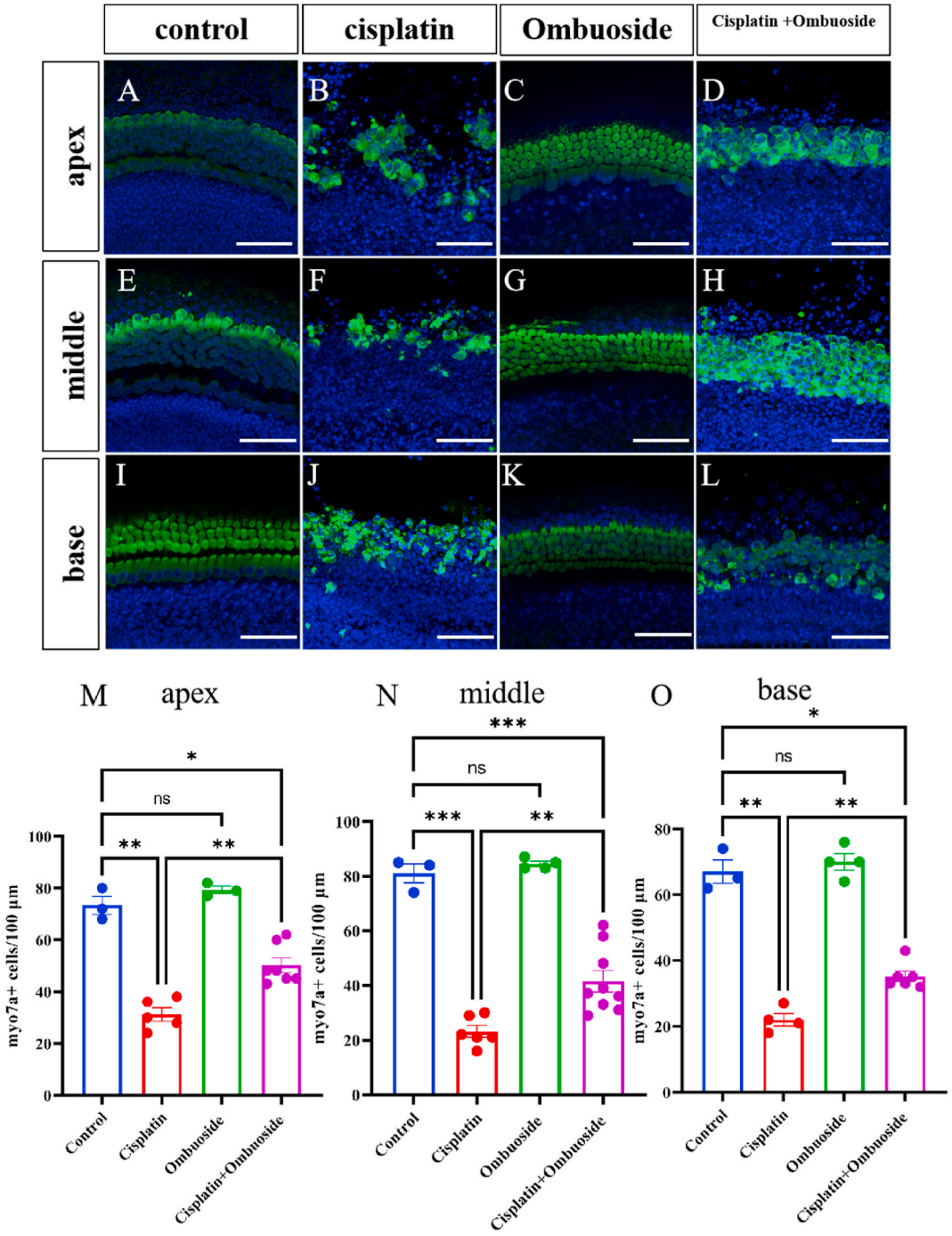


**Fig. 4.** Ombuoside protects against cisplatin-induced damage in cochlear hair cells. A–L. Myosin VII (green) and DAPI (blue) immunofluorescence staining in the apex (A–D), middle (E–H), and base (I–L) regions of the cochlea according to drug treatment, N ≥ 3. M–O. Counts of myosin VII-positive hair cells every 100 μm along the apex (M), middle (N), and base (O) regions of cochlear explants, N ≥ 3. Data are presented as mean ± SEM. *P ≤ 0.05, **P ≤ 0.01, ***P ≤ 0.001, and ****P ≤ 0.0001. Scale bar: 50 μm.

(base: 67.0 ± 3.60, middle: 73.4 ± 3.53, apex: 81.0 ± 3.51) (Fig. 4A–E, I). Therefore, ombuoside alone did not affect the shape and number of hair cells in the cochlear explants. In the cisplatin-treated group, the arrangement of the inner and outer hair cells in the cochlear explants was disrupted in the base, middle, and apex areas. Additionally, the number of hair cells was significantly reduced (base: 22.0 ± 1.87, middle: 23.2 ± 2.18, apex: 31.2 ± 2.58) (Fig. 4B–F, J). In contrast, co-treatment with ombuoside significantly reduced the hair cell loss (base: 35.2 ± 1.65, middle: 41.5 ± 3.96, apex: 45.4 ± 3.88) (Fig. 4D–H, L) caused by cisplatin, resulting in a significantly increased number of hair cells in the co-treatment group compared with that in the cisplatin group. These results indicate that ombuoside protected against cisplatin-induced hair cell damage.

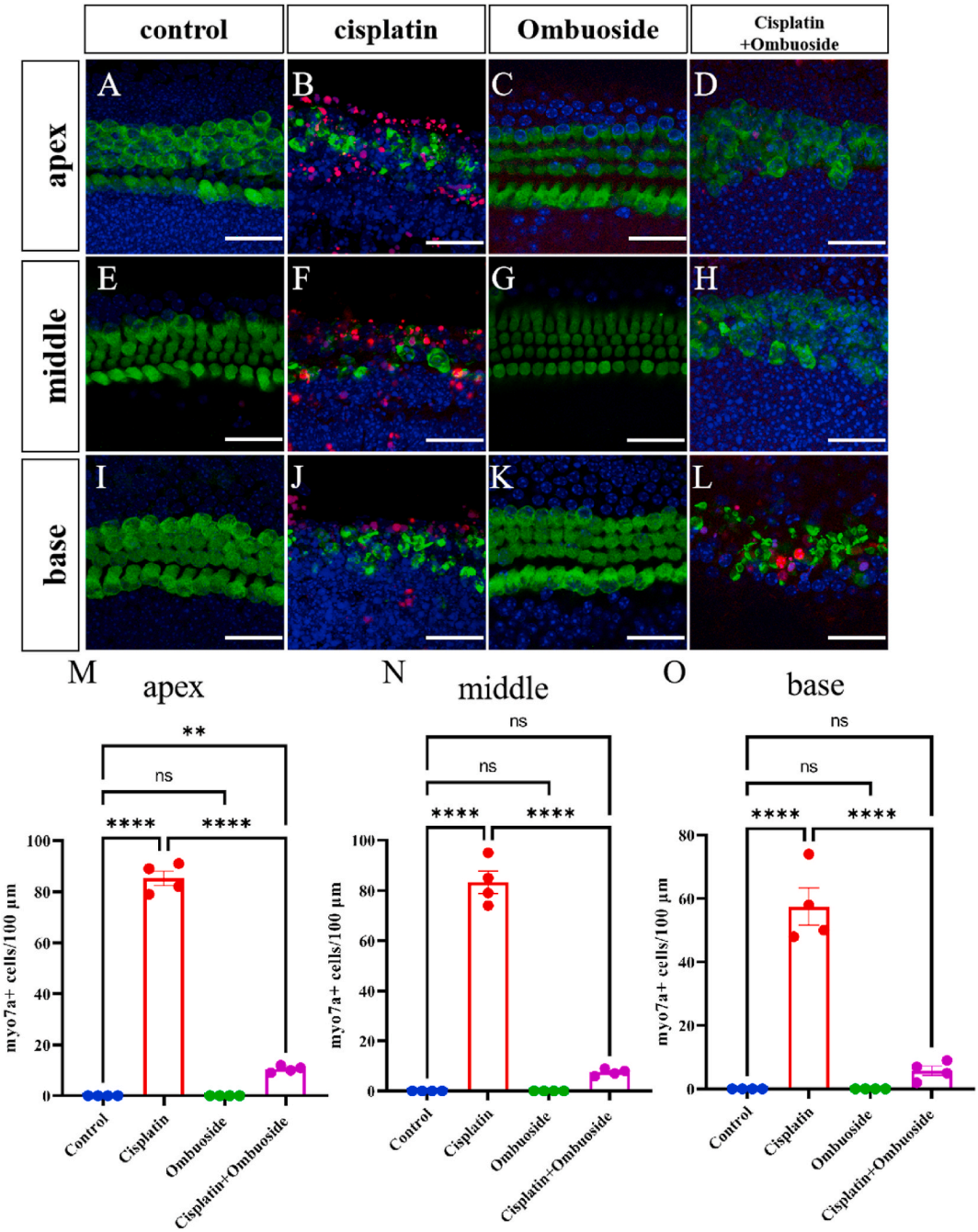


**Fig. 5.** Effects of ombuoside and cisplatin on apoptosis in cochlear explants. A–L. Detection of apoptotic cells in cochlear explants using terminal deoxynucleotidyl transferase dUTP nick end labeling (TUNEL) (red), and hair cells stained with myosin VII (green) in the apex (A–D), middle (E–H), and base (I–L) regions of the cochlea, N = 4. M–O. Counting of TUNEL-positive hair cells every 100 μm along the apex (M), middle (N), and base (O) regions of cochlear explants, N = 4. Data are presented as mean ± SEM. *P ≤ 0.05, **P ≤ 0.01, ***P ≤ 0.001, and ****P ≤ 0.0001. Scale bar: 25 μm.

Cisplatin-induced hair cell injury is primarily associated with hair cell apoptosis. We investigated whether ombuoside protected hair cells by inhibiting apoptosis. Hair cells were stained with myosin VIIa and apoptotic cells were detected using terminal deoxynucleotidyl transferase dUTP nick end labeling (TUNEL). The TUNEL assay revealed that cisplatin induced apoptosis of hair cells and treatment of cochlear explants with ombuoside significantly reduced apoptosis (Fig. 5). These results suggest that ombuoside reduced cisplatin-induced ototoxicity by inhibiting apoptosis in cochlear explants.

### 3.5. *Ombuoside protects zebrafish hair cells from cisplatin-induced damage*

We used zebrafish as the animal model to validate the potential protective effects of ombuoside against cisplatin-induced injury *in vivo*. The structure and function of zebrafish hair cells in the lateral line are similar to those of mammalian inner ear hair cells [46–48]. Additionally, many homologous genes related to human deafness are expressed in the hair cells of the zebrafish lateral line. The hair cells of zebrafish neuromasts are located on the surface of the fish body, thus, they are easy to manipulate and observe *in vivo* [48,49]. These characteristics make zebrafish an important research model for hair cell development. We treated *Tg(brn3c:GFP)* transgenic zebrafish, which were marked with green fluorescent proteins specifically expressed in hair cells, with cisplatin and/or ombuoside. Compared with the control group by IF, zebrafish treated with ombuoside showed no difference in the morphology or number of floral-shaped lateral neuromasts formed by hair cell aggregation (control: 10.38 ± 1.08 vs. ombuoside: 9.23 ± 0.89). After cisplatin treatment, the number of hair cells decreased drastically (3.05 ± 0.29), and the cells became irregular in shape. Co-treatment of cisplatin with 30 μmol/L ombuoside showed a protective effect on the hair cells of zebrafish neuromasts, resulting in a higher number of hair cells (5.84 ± 0.27) and more regularly shaped cells, compared with those in the cisplatin group (Fig. 6A–E).

Furthermore, RT-qPCR confirmed that the apoptosis-promoting genes *noxal, baxb,* and *tp53* were significantly upregulated after cisplatin treatment. Conversely, the expression of the apoptosis-inhibiting gene *bcl2a* was significantly decreased. When co-treated with ombuoside, the expression of *noxal, baxb,* and *tp53* was significantly decreased, whereas that of *bcl2a* was upregulated, compared with that in the cisplatin-treated group (Fig. 6F). These results revealed the protective effects of ombuoside against cisplatin-induced ototoxicity *in vivo*.

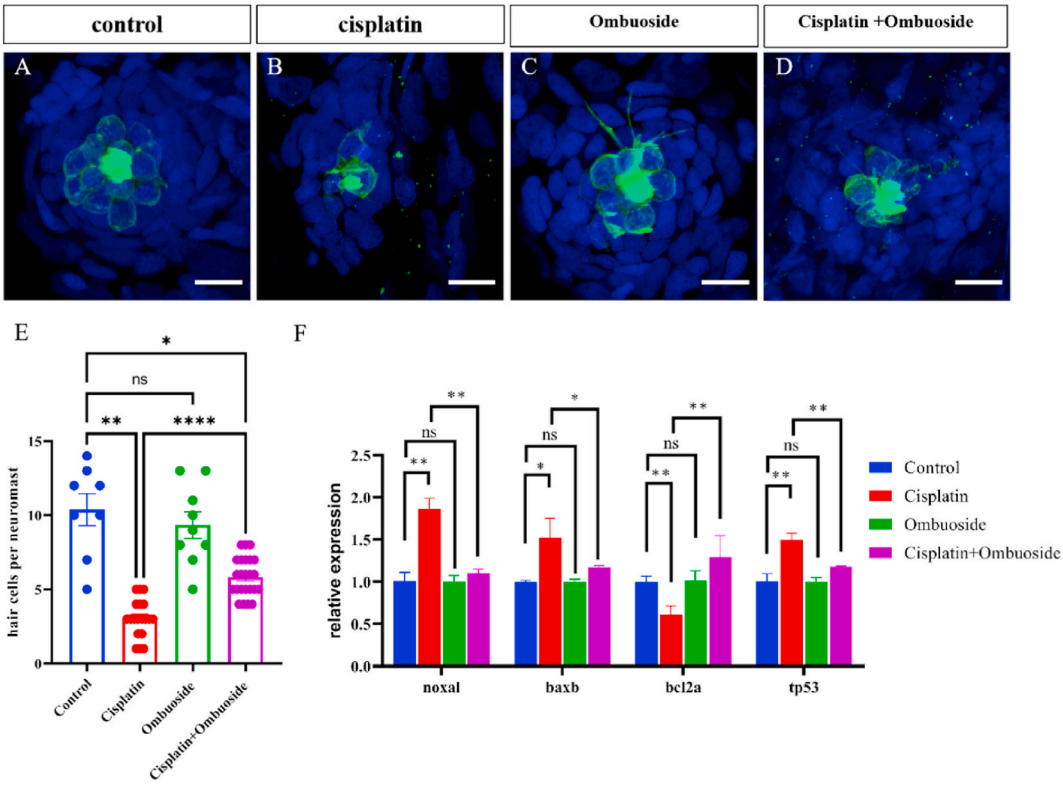


**Fig. 6.** Ombuoside protects zebrafish hair cells from cisplatin-induced damage. A–D. *Tg(brn3c:GFP)* Zebrafish larvae at 5 dpf were pre-exposed in ombuoside for 2 h, and then co-treated with 800 μmol/L cisplatin for 8 h. Confocal microscopy was used to detect the green fluorescent protein (GFP) expression of hair cells, N ≥ 8. E. Assessment of the number of hair cells per neuromast in Fig. .6A–D, N ≥ 8.F. Relative expression of apoptosis-associated mRNA in zebrafish treated with cisplatin alone or co-treated with ombuoside, N = 3. Data are presented as mean ± SEM. *P ≤ 0.05, **P ≤ 0.01, ***P ≤ 0.001, and ****P ≤ 0.0001. Scale bar: 10 μm.

## 4. Discussion

In this study, we demonstrated the protective effects of ombuoside against cisplatin-induced hair cell death. Ombuoside protected HEI-OCI cells from cisplatin-induced apoptosis. The abnormal expression of apoptosis-associated proteins, excessive ROS production, and mitochondrial membrane depolarization triggered by cisplatin can be significantly reduced by ombuoside. In mouse cochlear explants *in vitro* and zebrafish lateral neuromasts *in vivo*, the number of hair cells decreased and their shape deformed due to cisplatin. However, this effect was significantly attenuated by ombuoside treatment. These results suggest that ombuoside has a strong potential to safeguard hair cells from cisplatin-induced apoptosis by inhibiting ROS production and the mitochondrial apoptotic pathway. This suggests that ombuoside is a potential ear protector against drug-induced hearing loss.

Evidence suggests that cisplatin induces hair cell apoptosis, leading to ototoxicity [8,14,18]. Our results revealed that cisplatin treatment significantly induced apoptosis in hair cells, which was alleviated by simultaneous exposure to ombuoside. This provides evidence of the protective potential of ombuoside against cisplatin-induced hair cell damage. Various apoptotic pathways are involved in cisplatin-induced ototoxicity, including mitochondria-mediated apoptosis pathways [8,18]. The Bcl-2-family proteins, including the pro-apoptotic factors Bax, Bad, and Bid, as well as the anti-apoptotic factors Bcl-2, Bcl-x, and Bcl-w, are vital regulator of the mitochondria-mediated apoptosis pathways [40,41]. Bcl-2 inhibits apoptosis by preventing the release of cytochrome *c*, *a* central regulator of apoptosis, from the mitochondria into the cytoplasm. Conversely, Bad and Bax promote the release of cytochrome *c* from mitochondria and subsequently activate the caspase-mediated apoptotic pathway, resulting in cell apoptosis [50,51]. Our results showed that cisplatin treatment upregulated the expression of the pro-apoptotic proteins Bad and Bax, and significantly down-regulated the expression of the anti-apoptotic protein Bcl-2. However, co-treatment with ombuoside effectively reduced the effect of cisplatin on the expression of these apoptotic regulatory factors and reduced cisplatin-induced apoptosis in hair cells. Ombuoside protects PC12 cells from L-DOPA-induced neurotoxicity by inhibiting L-DOPA-induced continuous phosphorylation of ERK1/2 and JNK1/2, elevating caspase-3 expression and decreasing SOD activity, thereby acting as a neuroprotective drug [32]. In this study, we demonstrated that ombuoside can protect against ototoxicity. It effectively protects hair cells from cisplatin-induced apoptosis by inhibiting the activation of mitochondria-mediated apoptotic pathways.

Apoptosis of hair cells is the primary mechanism underlying cisplatin-induced ototoxicity. Excessive ROS disrupt normal hair cell function by triggering the mitochondrial release of cytochrome *c* and activating the caspase pathway, leading to hair cell apoptosis [12,13,15]. Our results suggest that pretreatment with ombuoside significantly reduces cisplatin-induced ROS production of HEI-OC1 cells, thereby reducing apoptosis. Our findings are consistent with ombuoside serving as a ROS scavenger, suggesting that the antioxidant properties of ombuoside may be the primary mechanism underlying its anti-apoptotic effects. As reported, antioxidants regulate ROS level by scavenging free radicals, we postulate that ombuoside may also functions in reducing intracellular ROS concentrations by eliminating excessive free radicals generated by cisplatin, thereby mitigating apoptosis.

Currently, the two main protective measures for reducing cisplatin-induced ototoxicity involve inhibiting the apoptotic pathway and enhancing the antioxidant protection system. The exogenous administration of antioxidants is a viable strategy to protect against cisplatin-induced ototoxicity. Flavonoids are a type of naturally occurring polyphenolic compounds ubiquitously present in photosynthetic cells [52]. These compounds serve as potent natural antioxidants, capable of neutralizing free radicals and mitigating oxidative stress-induced cellular damage. Such as hesperidin [53], quercetin [27], resveratrol [54], rutin [55], also exerted protective effects in cisplatin-induced rat ototoxicity models. Although various flavonoid drugs have been found to alleviate cisplatin-induced ototoxicity, none of them have been used in clinical treatment so far. Discovering more flavonoid drugs with this effect can provide more options for treatment plans aimed at reducing cisplatin-induced ototoxicity. In this study, we demonstrated that ombuoside prevented the excessive production of mitochondrial ROS caused by cisplatin, thereby alleviating mitochondrial dysfunction and cell apoptosis. Although ombuoside significantly alleviated cisplatin-induced damage, the number of hair cells was still reduced compared with those in the controls without cisplatin treatment. Therefore, we can take some measures to protect cochlear hair cells from drug-induced ototoxicity and maximize the protective effects of ombuoside, such as explore effective mitochondria-targeted antioxidants that can be co-administered with ombuoside, and administering intratympanic injections rather than ocular drug delivery. Despite the promising initial findings, further detailed *in vivo* animal experiments are needed to confirm the results of this study, and distortion product otoacoustic emission (DPOAE) or auditory brainstem response (ABR) will utilize to accurately assess the role of ombuoside in preventing cisplatin-induced ototoxicity. Future research on the precise mechanisms underlying the protective effect of ombuoside in alleviating cisplatin-induced ototoxicity in hair cells will help us to better understand the molecular mechanisms of hair cell survival and facilitate the development of improved therapeutic strategies for deafness induced by hair cell injury.

## 5. Conclusion

We demonstrated the significant protective effects of ombuoside against cisplatin-induced ototoxicity by blocking the ROS production and mitochondrial apoptotic pathways. Our findings revealed that ombuoside is a potential protective agent against hearing loss caused by ototoxic injuries. Further, they suggest that ombuoside, a natural flavonoid, can be used as a preventive or therapeutic agent for ototoxic injury-induced hearing loss. These results have significant implications for future clinical practice.

## CRediT authorship contribution statement

**Xingxing Wu:** Writing – review & editing, Writing – original draft, Validation, Software, Methodology, Investigation, Funding acquisition, Formal analysis, Conceptualization. **Xixia Peng:** Writing – review & editing, Validation, Methodology, Formal analysis.

**Yue Zhang:** Methodology. **Wanjun Peng:** Software, Investigation. **Xiaochan Lu:** Software, Formal analysis. **Tingting Deng:** Software, Funding acquisition. **Guohui Nie:** Writing – review & editing, Writing – original draft, Validation, Funding acquisition, Conceptualization.

## Informed consent statement

Not applicable.

## Institutional review board statement

Not applicable.

## Data availability statement

The data presented in this study are available on request from the corresponding author.

## Funding

This research was funded by National Natural Science Foundation of China (81970875, 82192865 and 82002936) Shenzhen Science and Technology Innovation Committee (JCYJ20230807115103007, LCYSSQ20220823091403007, JSGG20220606141001002, KCXFZ20201221173413038 and JCYJ20190806163209126), Shenzhen Portion of Shenzhen-Hong Kong Science and Technology Innovation Cooperation Zone (HTHZQSWS-KCCYB-2023060), Sanming Project of Medicine in Shenzhen (SZSM201612031) and Development and Reform Commission of Shenzhen Municipality.

## Declaration of competing interest

The authors declare that they have no known competing financial interests or personal relationships that could have appeared to influence the work reported in this paper.

## Appendix A. Supplementary data

Supplementary data to this article can be found online at https://doi.org/10.1016/j.heliyon.2024.e39166.

## References

[1] S. Chadha, K. Kamenov, A. Cieza, The world report on hearing, 2021, Bull. World Health Organ. 99 (4) (2021) 242.
[2] WHO [cited 2023 1/10]; Available from: https://www.who.int/news-room/fact-sheets/detail/deafness-and-hearing-loss, 2023.
[3] D. Wang, S.J. Lippard, Cellular processing of platinum anticancer drugs, Nat. Rev. Drug Discov. 4 (4) (2005) 307–320.
[4] T. Langer, et al., Understanding platinum-induced ototoxicity, Trends Pharmacol. Sci. 34 (8) (2013) 458–469.
[5] P. Ganesan, et al., Ototoxicity: a challenge in diagnosis and treatment, J Audiol Otol 22 (2) (2018) 59–68.
[6] T.G. Rivelli, et al., Cisplatin based chemoradiation late toxicities in head and neck squamous cell carcinoma patients, Discov. Med. 20 (108) (2015) 57–66.
[7] D.S. Lee, et al., Cisplatin exposure acutely disrupts mitochondrial bioenergetics in the zebrafish lateral-line organ, Hear. Res. 426 (2022) 108513.
[8] S. Sheth, et al., Mechanisms of cisplatin-induced ototoxicity and otoprotection, Front. Cell. Neurosci. 11 (2017) 338.
[9] J. Wu, et al., Programmed cell death pathways in hearing loss: a review of apoptosis, autophagy and programmed necrosis, Cell Prolif. 53 (11) (2020) e12915.
[10] X. Wang, et al., Cisplatin-induced ototoxicity: from signaling network to therapeutic targets, Biomed. Pharmacother. 157 (2023) 114045.
[11] Y.M. Choi, et al., Mechanism of cisplatin-induced cytotoxicity is correlated to impaired metabolism due to mitochondrial ROS generation, PLoS One 10 (8) (2015) e0135083.
[12] X. Guo, et al., Forskolin protects against cisplatin-induced ototoxicity by inhibiting apoptosis and ROS production, Biomed. Pharmacother. 99 (2018) 530–536.
[13] V. Ramkumar, et al., Oxidative stress and inflammation caused by cisplatin ototoxicity, Antioxidants 10 (12) (2021).
[14] Q. Tang, et al., Cisplatin-induced ototoxicity: updates on molecular mechanisms and otoprotective strategies, Eur. J. Pharm. Biopharm. 163 (2021) 60–71.
[15] T. Finkel, Signal transduction by reactive oxygen species, J. Cell Biol. 194 (1) (2011) 7–15.
[16] M.Z. Huang, J.Y. Li, Physiological regulation of reactive oxygen species in organisms based on their physicochemical properties, Acta Physiol. 228 (1) (2020) e13351.
[17] H. Sies, et al., Defining roles of specific reactive oxygen species (ROS) in cell biology and physiology, Nat. Rev. Mol. Cell Biol. 23 (7) (2022) 499–515.
[18] E. Gentilin, et al., Cisplatin-induced ototoxicity: updates on molecular targets, Trends Mol. Med. 25 (12) (2019) 1123–1132.
[19] R.A. Hazlitt, J. Min, J. Zuo, Progress in the development of preventative drugs for cisplatin-induced hearing loss, J. Med. Chem. 61 (13) (2018) 5512–5524.
[20] N.D. Doolittle, et al., Delayed sodium thiosulfate as an otoprotectant against carboplatin-induced hearing loss in patients with malignant brain tumors, Clin. Cancer Res. 7 (3) (2001) 493–500.
[21] D. Thomas Dickey, et al., Protection against cisplatin-induced ototoxicity by N-acetylcysteine in a rat model, Hear. Res. 193 (1–2) (2004) 25–30.
[22] M. Fouladi, et al., Amifostine protects against cisplatin-induced ototoxicity in children with average-risk medulloblastoma, J. Clin. Oncol. 26 (22) (2008) 3749–3755.
[23] M.A. Somdaş, et al., Protective effect of N-acetylcysteine against cisplatin ototoxicity in rats: a study with hearing tests and scanning electron microscopy, Braz J Otorhinolaryngol 86 (1) (2020) 30–37.
[24] Fda [cited 2023 1/10]; Available from: https://www.fda.gov/drugs/resources-information-approved-drugs/fda-approves-sodium-thiosulfate-reduce-risk-ototoxicity-associated-cisplatin-pediatric-patients, 2022.

[25] N.B. Gill, et al., Unveiling the role of oxidative stress in cochlear hair cell death: prospective phytochemical therapeutics against sensorineural hearing loss, Int. J. Mol. Sci. 25 (8) (2024).
[26] M. Ayaz, et al., Flavonoids as prospective neuroprotectants and their therapeutic propensity in aging associated neurological disorders, Front. Aging Neurosci. 11 (2019) 155.
[27] S.K. Lee, et al., Protective role of quercetin against cisplatin-induced hair cell damage in zebrafish embryos, Hum. Exp. Toxicol. 34 (11) (2015) 1043–1052.
[28] T. Mahesh, V.P. Menon, Quercetin allievates oxidative stress in streptozotocin-induced diabetic rats, Phytother Res. 18 (2) (2004) 123–127.
[29] H.S. Choi, et al., Anxiolytic effects of herbal ethanol extract from Gynostemma pentaphyllum in mice after exposure to chronic stress, Molecules 18 (4) (2013) 4342–4356.
[30] H.S. Choi, et al., Neuroprotective effects of herbal ethanol extracts from Gynostemma pentaphyllum in the 6-hydroxydopamine-lesioned rat model of Parkinson's disease, Molecules 15 (4) (2010) 2814–2824.
[31] K.S. Shin, et al., Gypenosides attenuate the development of L-DOPA-induced dyskinesia in 6-hydroxydopamine-lesioned rat model of Parkinson's disease, BMC Neurosci. 16 (2015) 23.
[32] U. Davaasambuu, et al., Ombuoside from Gynostemma pentaphyllum protects PC12 cells from L-DOPA-induced neurotoxicity, Planta Med. 84 (14) (2018) 1007–1012.
[33] J.M. Amaro-Luis, M. Adrián, C. Díaz, Isolation, identification and antimicrobial activity of ombuoside from Stevia triflora, Ann. Pharm. Fr. 55 (6) (1997) 262–268.
[34] S. Fahn, Description of Parkinson's disease as a clinical syndrome, Ann. N. Y. Acad. Sci. 991 (2003) 1–14.
[35] R. Wang, L.C. Shih, Parkinson's disease - current treatment, Curr. Opin. Neurol. 36 (4) (2023) 302–308.
[36] Y. He, et al., Inhibition of Protein arginine methyltransferase 6 reduces reactive oxygen species production and attenuates aminoglycoside- and cisplatin-induced hair cell death, Theranostics 10 (1) (2020) 133–150.
[37] X. Lu, et al., Novel application of eupatilin for effectively attenuating cisplatin-induced auditory hair cell death via mitochondrial apoptosis pathway, Oxid. Med. Cell. Longev. 2022 (2022) 1090034.
[38] S.M. Rocha-Sanchez, et al., Quinoxaline protects zebrafish lateral line hair cells from cisplatin and aminoglycosides damage, Sci. Rep. 8 (1) (2018) 15119.
[39] B. Nan, et al., Astaxanthine attenuates cisplatin ototoxicity in vitro and protects against cisplatin-induced hearing loss in vivo, Acta Pharm. Sin. B 12 (1) (2022) 167–181.
[40] C.F.A. Warren, M.W. Wong-Brown, N.A. Bowden, BCL-2 family isoforms in apoptosis and cancer, Cell Death Dis. 10 (3) (2019) 177.
[41] P.E. Czabotar, A.J. Garcia-Saez, Mechanisms of BCL-2 family proteins in mitochondrial apoptosis, Nat. Rev. Mol. Cell Biol. 24 (10) (2023) 732–748.
[42] M.C. Carou, et al., Apoptosis in ovarian granulosa cells of cattle: morphological features and clearance by homologous phagocytosis, Acta Histochem. 117 (1) (2015) 92–103.
[43] Y.R. Kim, et al., C-Phycocyanin from limnothrix species KNUA002 alleviates cisplatin-induced ototoxicity by blocking the mitochondrial apoptotic pathway in auditory cells, Mar. Drugs 17 (4) (2019).
[44] J.E. Ricci, R.A. Gottlieb, D.R. Green, Caspase-mediated loss of mitochondrial function and generation of reactive oxygen species during apoptosis, J. Cell Biol. 160 (1) (2003) 65–75.
[45] U. Al-Zubaidi, et al., The spatio-temporal dynamics of mitochondrial membrane potential during oocyte maturation, Mol. Hum. Reprod. 25 (11) (2019) 695–705.
[46] P.J. Atkinson, et al., Sensory hair cell development and regeneration: similarities and differences, Development 142 (9) (2015) 1561–1571.
[47] M. Holmgren, L. Sheets, Using the zebrafish lateral line to understand the roles of mitochondria in sensorineural hearing loss, Front. Cell Dev. Biol. 8 (2020) 628712.
[48] L. Sheets, M. Holmgren, K.S. Kindt, How zebrafish can drive the future of genetic-based hearing and balance research, J Assoc Res Otolaryngol 22 (3) (2021) 215–235.
[49] S. Baek, et al., Single-cell transcriptome analysis reveals three sequential phases of gene expression during zebrafish sensory hair cell regeneration, Dev. Cell 57 (6) (2022) 799–819.e6.
[50] A. Peña-Blanco, A.J. García-Sáez, Bax, Bak and beyond - mitochondrial performance in apoptosis, FEBS J. 285 (3) (2018) 416–431.
[51] A.Z. Spitz, E. Gavathiotis, Physiological and pharmacological modulation of BAX, Trends Pharmacol. Sci. 43 (3) (2022) 206–220.
[52] A.W. Boots, G.R. Haenen, A. Bast, Health effects of quercetin: from antioxidant to nutraceutical, Eur. J. Pharmacol. 585 (2–3) (2008) 325–337.
[53] J. Lou, et al., Hesperidin activates Nrf2 to protect cochlear hair cells from cisplatin-induced damage, Redox Rep. 29 (1) (2024) 2341470.
[54] C.H. Lee, et al., Dose-dependent effects of resveratrol on cisplatin-induced hearing loss, Int. J. Mol. Sci. 22 (1) (2020).
[55] S. Zheng, et al., The protective effect of rutin against the cisplatin-induced cochlear damage in vitro, Neurotoxicology 90 (2022) 102–111.